

Award Accounts

The Chemical Society of Japan Award for Creative Work for 2006

Molecular Self-Assembly into One-Dimensional Nanotube Architectures and Exploitation of Their Functions

Toshimi Shimizu

Nanotube Research Center (NTRC), National Institute of Advanced Industrial Science and Technology (AIST), Tsukuba Central 5, 1-1-1 Higashi, Tsukuba 305-8565

Received July 8, 2008; E-mail: tshmz-shimizu@aist.go.jp

This review article focuses on the self-assembly of amphiphilic molecules into discrete, hollow cylindrical tubular architectures (organic nanotubes). Research on nanotube formation from dumbbell-shaped peptide lipids, 1-*O*-glucopyranoside and 1-*N*-glucopyranosylamide lipids, and wedge-shaped bolaamphiphilic glycolipids with carboxylic, amino, or oligoglycine groups at one end has been outlined with their characteristic self-assembly. Finally, recent progress in mass production, dimension control, and novel functions of organic nanotubes are described.

1. Introduction

Tobacco Mosaic Virus (TMV) is well-known as a typical example of naturally occurring nanotubes, which forms a perfect tubular architecture featured by its hollow cylindrical morphology and homogeneous dimensions.[1] On self-organization of TMV, RNA contributes a high-aspect-ratio core to template the helical self-assembly of 2130 identical proteins, resulting in a tubular assembly with definite dimensions (Figure 1a). Bottom-up self-organization of protein molecules as building blocks in this way produces a variety of virus morphologies including spheres, rods, and tubes. On the other hand, top-down microfabrication of semi-conductors will even now hardly fabricate hollow cylindrical structures with diameters of less than 1 μm. However, certain amphiphilic or self-assembling molecules, whose structures are rationally designed, can self-assemble into tubular morphologies in a way similar to TMV, and yet without depending on templates.[2–5] A large number of nanotube objects including carbon and metal nanotubes are currently obtainable based on not only one-dimensional growth of a certain atom species,[6–8] but also on formation using nanoporous templates.[9,10] Formation of organic nanotubes on the basis of molecular self-assembly differs from those methodologies. Possible molecular shapes and spatial arrangement of each functional group, and the local environment of solvophilic and solvophobic moieties allow us to produce a variety of discrete organic nanotubes, together with different types of self-assembly strategy.[2,11]

We have been investigating the self-assembly behavior of synthetic amphiphilic molecules that append sugar,[12–18] peptide,[19–21] and nucleic acid moieties[22–26] as hydrophilic headgroups.[27] Those structural components in nature are well-known to form diverse and multiple hydrogen-bond networks.

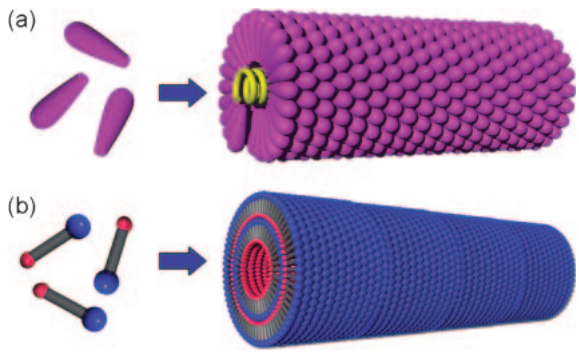

Figure 1. Schematic illustration for the self-assembly of (a) a protein and (b) an amphiphilic molecule into TMV and an organic nanotube, respectively.

Consequently, we developed unique one-dimensional structures including twisted or coiled nanofibers.[12] We also demonstrated dimension and morphology control of the nanofibers, the elucidation of molecular packing, and novel functions specific to the nanostructures.[23,28,29] Nano- and microtube formation with sugar- or peptide-based amphiphiles coincidentally took place on the occasion of a large number of self-assembling experiments.[19,30] Very recently, advanced functional organic nanotubes with different inner and outer surfaces have been produced and exhibited unique encapsulation, transport, and release properties of biomacromolecules as guests (Figure 1b).[31–33] Here we describe the effect of optimized molecular structures as tube-forming compounds on the size dimensions of resultant self-assembled nanotubes. We also address the morphological control of the organic nanotubes as well as the encapsulation behavior of guest molecules.

Published on the web December 12, 2008; doi:10.1246/bcsj.81.1554

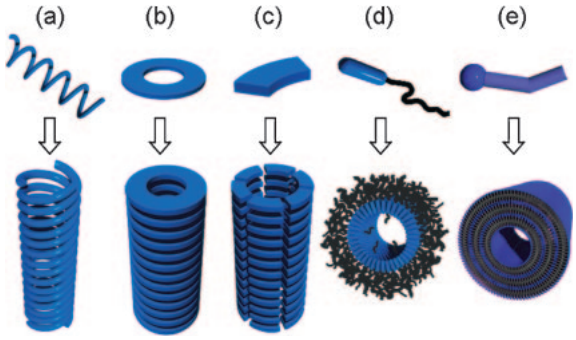

Figure 2. A variety of molecular building blocks that can self-assemble to form tubular architectures. (a) Helical chains, (b) rings, (c) dendrons, (d) block copolymers, and (e) general amphiphiles.

2. Self-Assembled Organic Nanotubes

2.1 Molecular Building Blocks for Nanotube Formation. Both well-defined hollow cylinder structures with nm-scale diameters and two opened ends are characteristic of discrete nanotubular architectures consisting of molecules.[2,11] Self-assembling strategy for such organic nanotubes from molecules may be classified into several categories, depending on a variety of molecular shapes of molecular building blocks (Figure 2). β-1,3-Glucan polysaccharides such as schizophyllan and curdlan form a triple helix to give a one-dimensional tubular structure in polar solvents like water (Figure 2a).[34–36] This feature gives the first category of a nanotubular host that can encapsulate carbon nanotubes,[37] polyaniline,[38] and diacetylene monomers.[39] If cyclic molecules such as cyclic peptides or cyclodextrin stack up and down with a shared central axis, the resultant molecular assemblies should provide tubular architectures (Figure 2b).[40–44] Otherwise, dendron molecules with a fan-like shape could form cyclic structures (rings) stabilized by complementary intermolecular interactions. The resultant rings can stack to give tubular morphologies (Figure 2c).[45–47] A unique advantage of these second and third strategies is the ability to control inner and outer diameters depending on the dimension of each cyclic molecule or ring. Disadvantageously, one has to pay in this case precise attention to molecular design in order for the participating functional groups of the molecule to take appropriate orientation and arrangement.[11]

On the other hand, hollow cylindrical or cochleated monolayer- or bilayer-membranes, consisting of polymer or low-molecular weight amphiphiles, can shape the tubular architectures (Figures 2d and 2e).[2] It should be noted that these nanotubes possess high-aspect ratios (diameter-to-length ratios) up to more than 10^4 and eventually provide well-dispersed fibrous structures with well-defined dimensions in solutions. Typical driving forces for the organization of such nanotubes are van der Waals force between hydrophobic long chains, as well as hydrogen bonds, coordination bonds, and π–π stacking between hydrophilic headgroups.

2.2 Formation Mechanism of Nanotubes from Amphiphiles. Amphiphilic molecules can be designated as self-assembling molecules that have both hydrophilic and hydrophobic moieties in the same molecule. When the amphiphile is dispersed in water, the resultant self-assembled morphology should be predictable by a critical packing parameter that means a size balance between the hydrophilic and hydrophobic regions.[48] This guiding principle in molecular self-assembly is in particular applicable when the long hydrocarbon chain as a hydrophobic part is in a liquid crystalline state. In connection with this theme, Kunitake's and Fuhrhop's research groups have achieved pioneering and extensive studies of molecular assemblies.[3,5,49] Consequently, they demonstrate experimentally that not only molecular orientation but also strong intermolecular interactions are critical to discuss the resultant self-assembled morphologies.

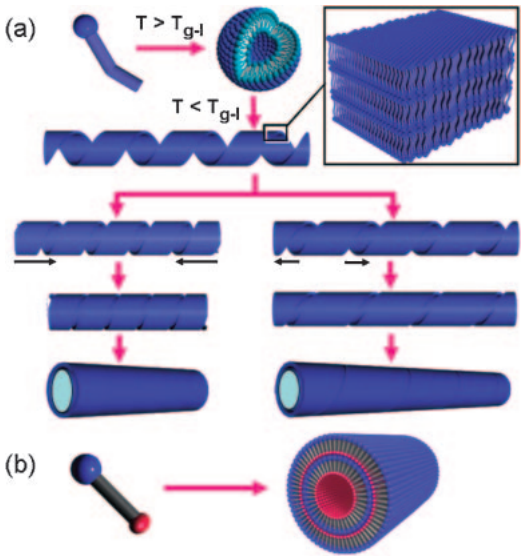

Figure 3. Two different possible formation schemes for self-assembled nanotubes. (a) Chiral molecular self-assembly and (b) packing-directed self-assembly. T_{g-l} means a gel-to-liquid crystalline phase transition temperature of each amphiphile.

Currently two different types of formation mechanism have been reported to feature the tubular architectures that self-assemble from low-molecular-weight amphiphiles (Figure 3).[2] When the aqueous dispersion of a chiral amphiphile is heated to temperatures above its gel-to-liquid crystalline phase transition temperature (T_{g-l}), it produces spherical micellar or vesicular assemblies of the amphiphiles. Gradual cooling of the aqueous dispersion beyond the T_{g-l} value induces morphological conversion from the spheres to coils with a definite handedness, depending on the intrinsic chirality of the amphiphilic molecule. Under these conditions, the molecular packing in a fluid state changes into a solid. The resultant coiled ribbons based on solid bilayer membranes slowly convert into tubular structures in a few days up to several weeks while reducing the pitch length of the ribbon or widening the ribbon width (Figure 3a).[50] Chiral molecular packing in the solid state is responsible for this formation mechanism.[51,52] At almost the same time in 1984, three independent research groups in the USA and Japan first found the formation of lipid nanotubes on the basis of this chiral molecular self-assembly.[50,53,54] The self-assembled nanotube formation from the glucoside and glucosamide lipids described later is based on this mechanism. The second growing mechanism of self-assembled

nanotubes has been reported for a limited number of examples. One of the characteristics is to lack the formation of intermediate chiral assemblies, producing directly tubular structures in a single step (Figure 3b). Wedge-shaped amphiphiles are found to undergo this packing-directed self-assembly to result in nanotubes based on the unique molecular shape.[31,55] The details are shown in the Section **5**.

3. Microtube Formation from Dumbbell-Shaped Peptide Amphiphiles

Dumbbell-shaped peptide amphiphiles **1**(*n*), **2**(*n*), and **3**–**6** (Chart 1) with dicarboxylic acids at both ends were synthesized, in which two oligopeptide moieties consisting of 1 to 3 amino residues as hydrophilic regions are connected covalently to both ends of long alkyl chains.[21] The self-assembly of the sodium salt of **1**(10) or **2**(10) in weakly alkaline aqueous solutions proved to produce tubular structures of 1–3 μm in outer diameter with closed ends.[19] We found that the resultant microtubes several hundred μm long encapsulate spherical molecular assemblies inside the tubes (Figure 4a). The vesicle-encapsulated microtubes displayed unique thermodynamic and mechanical stability since the tubular morphologies are still retained even at boiling temperatures or on sonication. Detailed FTIR and pH titration analyses showed that intralayer and intermolecular hydrogen bonds between acid–anion terminal carboxylic acids contribute to stabilize the bilayer membrane wall of the microtubular structures (Figure 4b).[21] High-resolution atomic force microscopy revealed that the peptide headgroups pack in a distorted hexagonal fashion arranging parallel to the normal of the microtube membrane surfaces (Figure 4c).[56] These findings are well compatible with the view that the oligoglycine residues form so-called polyglycine II-type hydrogen-bond networks with the nearest neighboring 6 molecules.[20,57,58] On the other hand, the dumbbell-shaped amphiphiles possessing the L-Val–L-Val residue as a hydrophilic region, which forms typical β-sheet hydrogen bonding, only self-assembled into nanofibers.[59,60] It should be noted that they never form tubular structures.

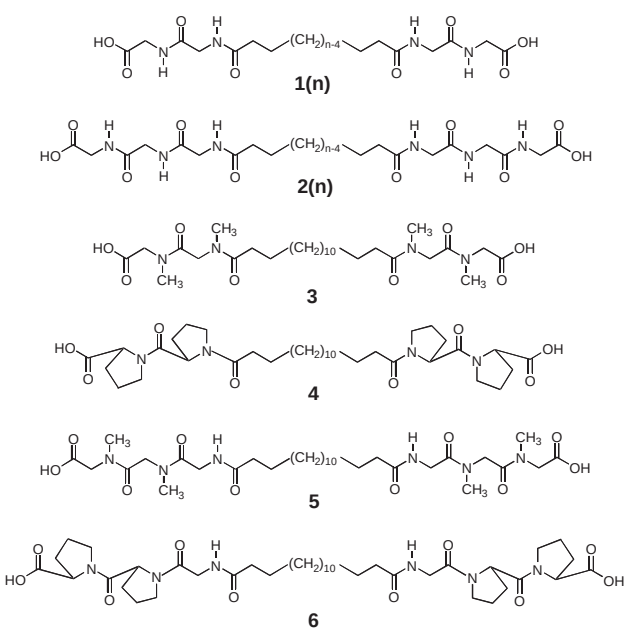

Chart 1.

4. Single-Head–Single-Tail-Type Glycolipids

4.1 Nanotube Formation from 1-*O*-Glucoside Glycolipids. A mixture of four 1-*O*-glucoside-type glycolipids [**7**: **7a**/**7b**/**7c**/**7d**, (5/50/16/29, w/w/w/w) (Chart 2)] were synthesized by linking the glucose moiety as a hydrophilic region with a meta-substituted long chain phenol[61] as a hydrophobic region, which is a main component of the renewable plant-derived resource cashew nut shell liquid (CNSL).[30] Refluxing the aqueous dispersion of **7** at 100 °C for 1 h and subsequent gradual cooling to room temperature resulted in the reproducible formation of organic nanotubes through molecular

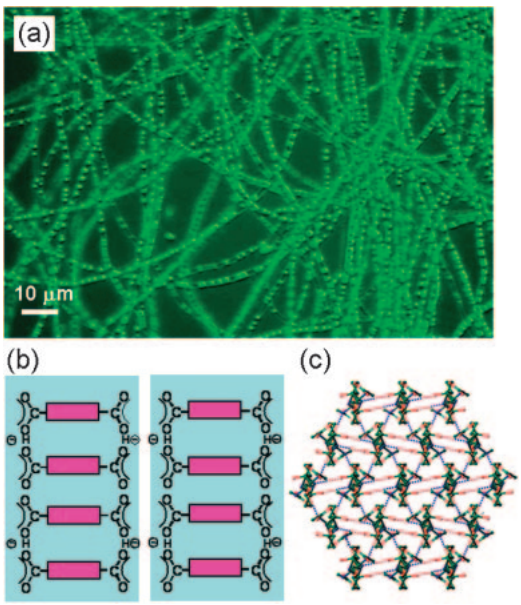

Figure 4. (a) Dark-field optical micrograph of vesicle-encapsulated microtubes from **1**(10). (b) Schematic illustration for the stabilization by intralayer and intermolecular hydrogen bonds between acid–anion terminal carboxylic acid. (c) A polyglycine II hydrogen-bond network.

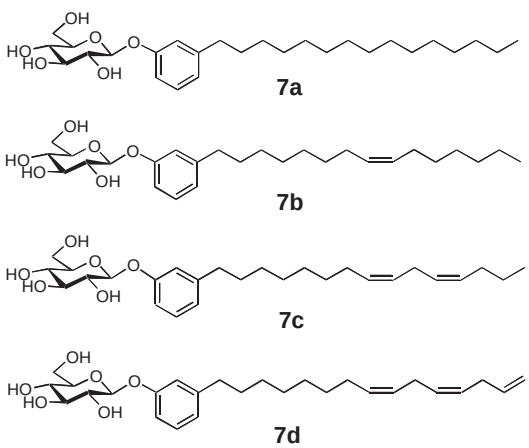

7a(~5%) / **7b**(~50%) / **7c**(~16%) / **7d**(~29%) : **7**

Chart 2.

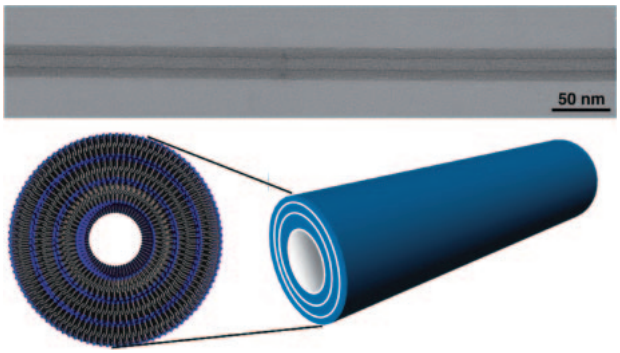

Figure 5. TEM image and plausible molecular packing for the self-assembled lipid nanotube from the glycolipid mixture **7**.

self-assembly.[30] The dimensions of the resulting nanotubes are 40–50 and 10–15 nm in outer and inner diameters, respectively. Although the inner diameters well correspond to those of multi-wall carbon nanotubes (MW-CNT), those dimensions give the smallest class of inner diameters among the lipid nanotubes obtained so far.[2] Powder X-ray diffraction (XRD) analyses revealed that the membrane walls of the nanotubes consist of 3–4 bilayer membranes of 3.1-nm thickness with an interdigitated structure (Figure 5).

To clarify the self-assembly and thermodynamic properties of each single component of **7**, we carefully fractionated the mixture of glycolipids **7** into constituting four components; saturated **7a**, monoene **7b**, diene **7c**, and triene **7d** by medium-pressure column chromatography.[28] T_{g-l} of **7c** and **7d** was found to be 17 and $-25\,^{\circ}C$, respectively, suggesting that the resultant solid nanotubes at room temperature include no glycolipids of **7c** and **7d**. These findings also indicate that the monoene component **7b** with a single cis double bond is critical for **7** to self-assemble into tubular architectures. Then, we investigated systematically the relationship between the unsaturation degree in the hydrocarbon chains and the ability of nanotube formation. For that purpose, we synthesized a series of novel glucopyranoside lipids **8**–**11** (Chart 3), which possess para-substituted, unsaturated long-chain alkanoylamino–phenol derivatives and eventually should give relatively higher T_{g-l} values.[62] The number of the cis double bonds, which were introduced into the oligomethylene chains, was varied as 0, 1, 2, and 3. The increase in the introduction number of the cis double bonds caused more facile self-assembly of the molecule into nanotubes.[63] Thus, appropriate number of cis double bonds is at least one critical structural factor to self-assemble into nanotubes in high efficiency.

4.2 Nanotube Formation from 1-*N*-Glucosamide Glycolipids. In order to obtain self-assembled organic nanotubes exclusively with homogeneous dimensions, we attempted to further optimize the molecular structure of glycolipids as tube-forming amphiphiles. The phenol moiety of the glycolipid component **7b** was replaced with an amide linkage in order to improve the relatively low T_{g-l} value ($=41\,^{\circ}C$) of **7b**. We thus designed and synthesized 1-*N*-glucosamide glycolipids **12**–**15** (Chart 4), in which the introduction position of the cis double bond was varied from the C6 to C11 carbons in the tetradecanoyl chain.[64] All the amphiphiles were easily synthesized in two steps without protecting the hydroxy groups.

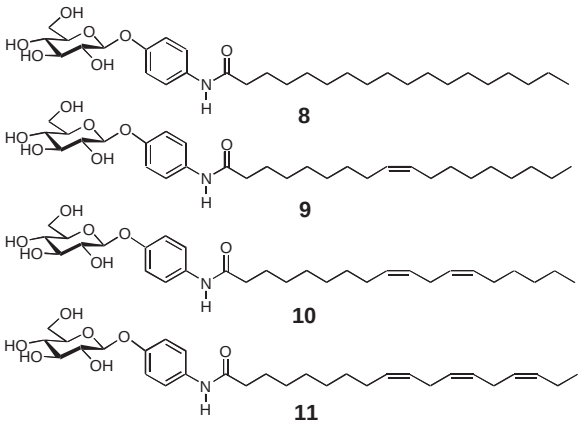

Chart 3.

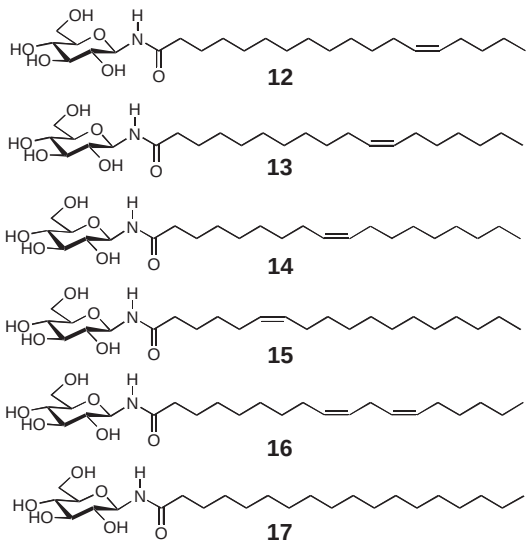

Chart 4.

The self-assembling behavior of each 1-*N*-glucosamide glycolipid was examined in aqueous solution. We also synthesized the diene derivative **16** as well as saturated **17** (Chart 4).[64]

We added the solid powder of **12**–**17** into water and refluxed the aqueous dispersion at $100\,^{\circ}C$ until the solution was transparent. Cooling the aqueous dispersions caused self-assembly of the glycolipids, producing nanotube structures only from glycolipids **12**, **13**, and **14**. In particular glycolipid **13** can give organic nanotubes on self-assembly in almost 100% yields (Figures 6a and 6b).[64] The T_{g-l} values for the obtained glycolipids increased in the order of **16** $< 50\,^{\circ}C <$ **14** $<$ **13** $<$ **12** $< 100\,^{\circ}C <$ **17**. The value of **15** was not determined. The CD spectra of each nanotube that self-assembled from **12**, **13**, and **14** showed negative Cotton effect around 234–236 nm at temperatures below the T_{g-l} value of each. The CD band intensity at 235 nm increased in the order of **14**, **12**, and **13** at $25\,^{\circ}C$ (Figure 6c). This order correlates well with the tendency in uniformity of the outer diameters mentioned below. This also suggests that the constituting molecules take the most remarkable chiral packing in a solid state.[52,65,66]

4.3 Uniformity of Outer Diameters. We found that through the self-assembly experiments of **12**–**17** both the number and incorporation position of the cis double bond have a

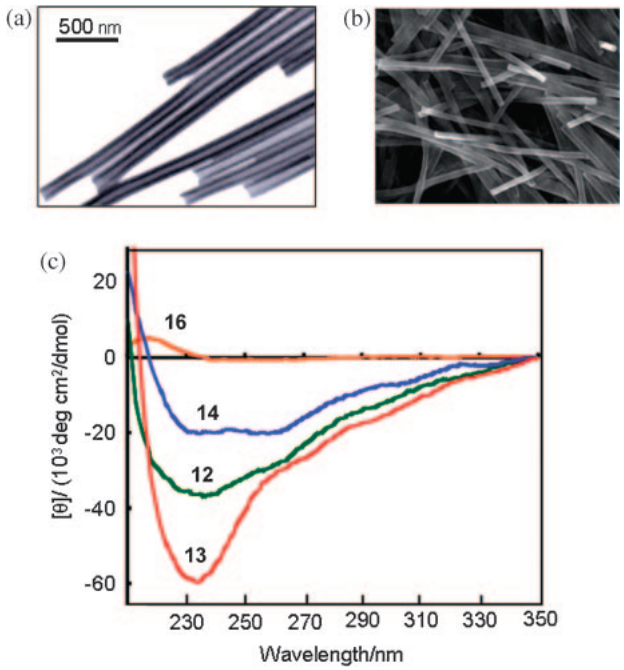

Figure 6. (a) TEM and (b) SEM images for the self-assembled lipid nanotubes from the glycolipid **13**. (c) CD spectra of the self-assembled lipid nanotubes from the glycolipids **12**, **13**, **14**, and **16** in water.

remarkable influence on the size-distribution of outer diameters for the self-assembled organic nanotubes. Therefore, we selected approximately 250 discrete organic nanotubes from **12**, **13**, and **14** in several TEM images to evaluate the average values for the outer and inner diameters, and their standard deviations. Consequently, the glycolipid nanotubes of **13** gave considerably homogeneous dimensions, of which the outer diameter particularly shows the narrowest size distribution (average: 200 nm, standard deviation: 23 nm) among three organic nanotubes from **12**, **13**, and **14**.[64] It has been reported experimentally and theoretically that chiral amphiphiles tend to pack at non-zero angles with nearest neighbors and eventually to result in coiled or tubular molecular assemblies.[51,67,68] The CD results mentioned above support that a bent structure of the glycolipid **13** has a relatively stronger tendency to form chiral molecular packing as compared with that of **12** and **14**.[66] The nanotube structures thus form in such a way that the solid bilayer membranes coil into helical ribbons and subsequently the helical pitch of the ribbon reduces or the helical ribbon width widens (Figure 3a).

5. Nanotube Formation from Wedge-Shaped Bolaamphiphilic Glycolipids

5.1 Wedge-Shaped Glycolipids with a Carboxylic Group at One End. Most self-assembled organic nanotubes from synthetic amphiphiles possess identical functional groups at inner and outer surfaces, since most of tube-forming amphiphiles form a bilayer structure with the same functionalities exposed to an external environment.[2] Wedge-shaped amphiphiles, in which two hydrophilic moieties of different size are covalently linked to the two ends of a hydrophobic spacer, possibly give two types of polytype depending on the molecular packing of

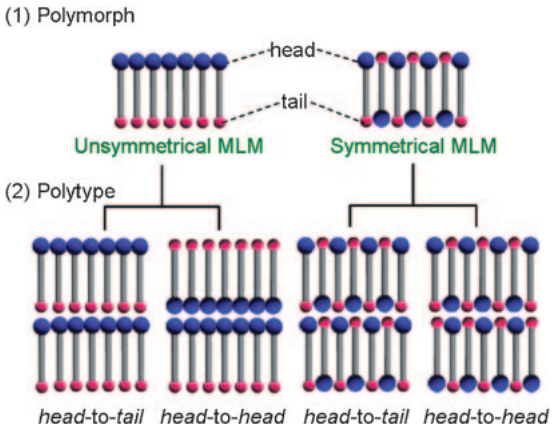

Figure 7. Four possible types of monolayer lipid membranes (MLMs) from wedge-shaped bolaamphiphiles.

symmetrical and unsymmetrical monolayer membranes.[69] An additional two types of polymorph depending on the stacking motif of each monolayer membrane (head-to-head and head-to-tail) result in at least four different types of monolayer membranes (Figure 7). If one can construct only the unsymmetrical monolayer membrane with a head-to-tail stacking exclusively among the four types, one can provide organic nanotubes having inner and outer surfaces covered with different functional groups.[70] We started to synthesize wedge-shaped amphiphiles **18**(*n*) with a relatively large glucose moiety and smaller carboxylic group at each end, which corresponds to asymmetric single-chain bolaamphiphiles.[71] The self-assembly of the amphiphiles **18**(*n*) with a variety of oligomethylene chains produced a mixture of two types of nanotubes, which have different outer diameters of approximately 30 and 200 nm.[31] The obtained relatively smaller and larger nanotubes are easily separable by conventional centrifugation (2000 G, 30 min at 15 °C) (Figure 8a). Powder X-ray analyses revealed that the isolated smaller and larger nanotubes consist of at least a single and three kinds of monolayer membrane motifs, respectively. We succeeded in obtaining single crystal X-ray structures for **18**(12) and **19** (Chart 5).[69,71] By using powder XRD, we also analyzed carefully a number of self-assembled nanotubes and nanotapes from a series of wedge-shaped amphiphiles. Taking all the obtained data into consideration, we found a determinate rule that each molecular packing motif can be predictable by the relationship between the long-range periodicity (*d*) of monolayer membranes and the extended molecular length (*L*) evaluated from molecular modeling.[31] The obtained *d* values for the smaller nanotubes were almost equal to *L*, showing that the MLM type is unsymmetrical with a head-to-tail interface. Thus, the self-assembled nanotubes with 30-nm diameters from **18**(14)–**18**(20) proved to be based on the unsymmetrical monolayer membrane with a parallel molecular packing.

5.2 Precise Control of Inner Diameters. Depending on the difference in the size of two terminal headgroups, the unsymmetrical monolayer membrane of the wedge-shaped amphiphiles bends spontaneously and eventually results in tubular morphologies. This packing-directed self-assembly is basically characteristic of the wedge-shaped amphiphiles. Simple mathematical analyses using a simulated molecular packing model

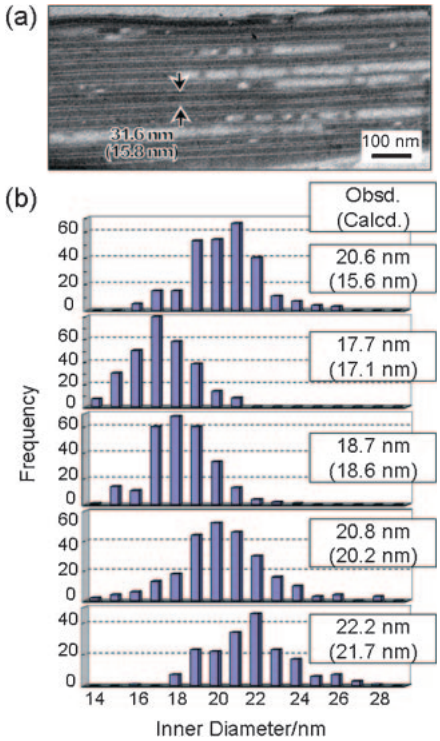

Figure 8. (a) TEM image of the self-assembled lipid nanotubes from **18**(16). (b) The histograms of inner diameters observed for the self-assembled lipid nanotubes from **18**(12), **18**(14), **18**(16), **18**(18), and **18**(20) from the top. Calculated inner diameters based on a simulation are also shown in parentheses.

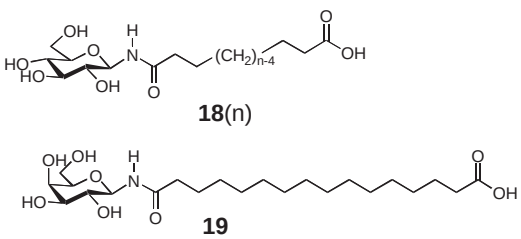

18(n)

19

Chart 5.

allowed us to induce the eq 1, showing that the inner diameter (D) is proportional to the molecular length (L) if the cross section area (a_l and a_s) of the two headgroups remains constant.[31] The D values of this type of nanotube should be controllable by changing the molecular length (L), namely, the carbon number of the oligomethylene spacers. The cross section area (a_l and a_s) is obtainable from single crystal X-ray analyses of the analogues as well as the areas per molecule in the Langmuir–Blodget film. The molecular modeling enables us to easily evaluate the molecular length (L).

$$D = 2a_sL/(a_l - a_s) \quad (1)$$

By putting all the related values into eq 1, we were able to calculate the inner diameter (D) for each separated smaller nanotube from the wedge-shaped bolaamphiphile **18**(n) ($n = 12$, 14, 16, 18, and 20). We also depict histograms on the basis of the experimentally obtained inner diameters for

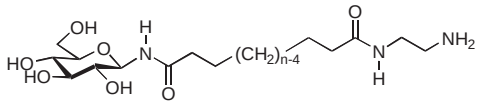

20(n)

Chart 6.

250 nanotubes in the TEM images (Figure 8b).[31] It should be noted here that well developed penetration of the staining reagent phosphotungstate into the hollow cylinder enables us to directly measure the inner diameter. Except for **18**(12), the observed values indeed increased in line with eq 1 with increasing spacer length of **18**(14), **18**(16), **18**(18), and **18**(20) bolaamphiphiles. Furthermore, the observed values are in good agreement with the calculated ones. These results indicate that the unsymmetrical monolayer membranes actually form with a head-to-tail motif in a way similar to the simulated molecular packing model for the calculation. Consequently, we first demonstrated that one can regulate the inner diameters of the self-assembled nanotubes at intervals of 1.5 nm on average by lengthening the oligomethylene spacer by two carbon atoms.

5.3 Wedge-Shaped Glycolipids with an Amino Group at One End. Controlling the polymorphism of molecular packing proved to be actually difficult in the self-assembly of the wedge-shaped glycolipids **18**(n) since two types of organic nanotubes with largely different outer diameters formed.[31] We recently succeeded in the selective control of polymorphism by optimizing the spacer length of wedge-shaped bolaamphiphiles, leading to the formation of a single species of organic nanotube based on an unsymmetrical monolayer membrane with a head-to-tail stacking motif.[32,55,72] A novel type of wedge-shaped glycolipids **20**(n) (Chart 6) were designed and synthesized, in which ethylenediamine moiety was linked to the carboxylic terminal of **18**(n). The self-assembly of a film-like solid of **20**(n), which was obtained by evaporation of the DMF solution, was observed to produce one-dimensional molecular assemblies, depending on the spacer length (n).[32] Namely, the glycolipids **20**(n) gave nanotubes and nanotapes for $n = 18$ and 20, and for $n \leq 17$, respectively (Figures 9a and 9b, each left image). When the carbon number of the spacer is $n \leq 17$, the CH_2 scissoring band gives two sets of IR bands ascribable to an orthorhombic perpendicular subcell structure of alkyl chains (Figures 9a and 9b, each right figure). In the case of $n = 18$ and 20 a single IR band ascribable to triclinic or monoclinic parallel subcell structure is observable. Furthermore, the small angle XRD for each nanotube showed a single reflection peak, supporting a lamellar structure based on the monolayer membrane. In particular, we found that the obtained long-range periodicity is slightly larger than the extended molecular length for $n \leq 17$, whereas shorter than those for $n = 18$ and 20 (Figure 10). These findings strongly support that the resultant nanotubes from **20**(18) and **20**(20) consist of unsymmetrical monolayer membranes with amino and glucose groups at the inner and outer surfaces, respectively. In other words, unique organic nanotubes with different inner and outer surfaces turn out to be exclusively obtainable via optimized self-assembly of rationally designed amphiphiles. It should also be noted that by controlling the pH values of aqueous dispersions during self-assembly we can obtain two types of

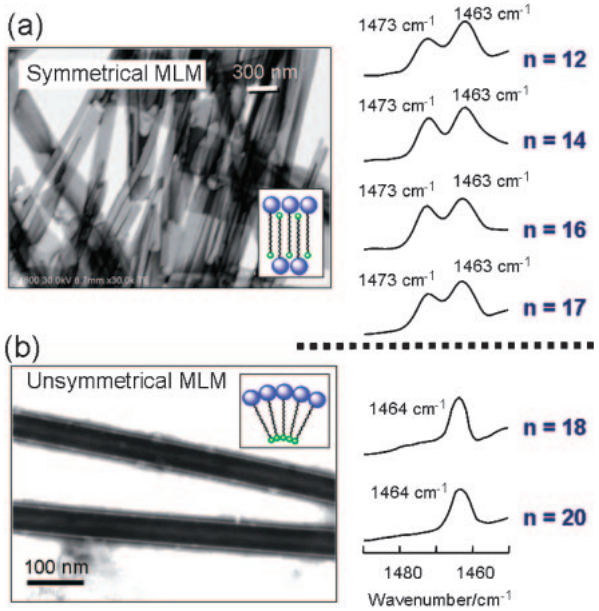

Figure 9. STEM images and the CH_2 scissoring IR bands for (a) the self-assembled nanotapes and (b) nanotubes from **20**(*n*). The STEM images are shown for the nanotapes from **20**(16) and **20**(20), respectively.

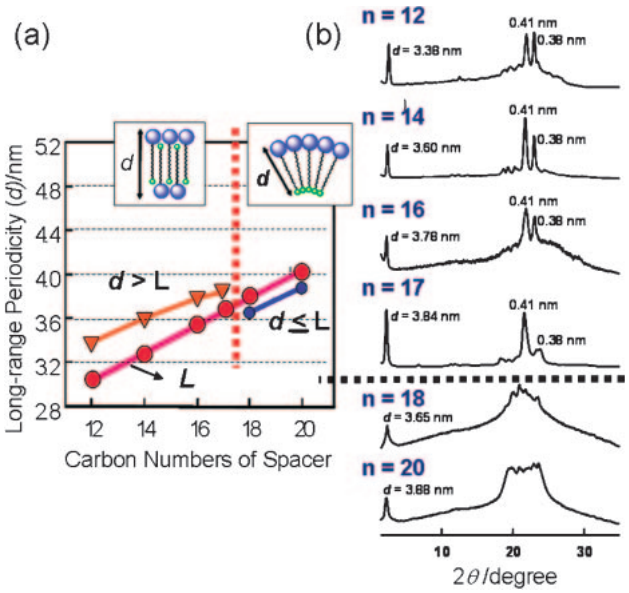

Figure 10. (a) The monolayer membrane (MLM) stacking periodicities (*d*) of the self-assembled nanotapes and nanotubes, which were estimated by XRD, plotted against the chain length of the oligomethylene spacer. The extended molecular length (*L*) of **20**(*n*) is also plotted. (b) XRD patterns of the self-assembled nanotapes and nanotubes from the short chain **20**(*n*) ($n = 12$, 14, 16, and 17) and long chain **20**(*n*) ($n = 18$ and 20), respectively.

organic nanotubes independently with 20–25 and 70–80 nm inner diameters.[32]

5.4 Wedge-Shaped Glycolipids with an Oligoglycine Moiety at One End. To further stabilize unsymmetrical monolayer membranes by fixation of the participating molecules, we attempted to examine the possibility of non-covalent stabi-

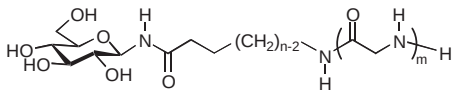

21(n,m)

Chart 7.

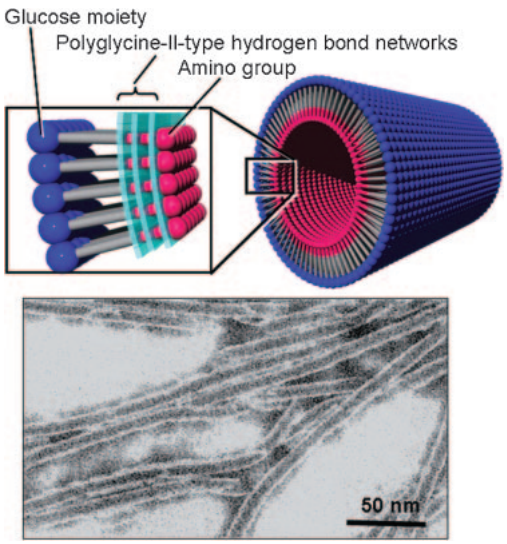

Figure 11. TEM image of the self-assembled lipid nanotubes from **21**(11,3) and their possible molecular packing.

lization through the formation of a two-dimensional hydrogen-bond network around the inner surfaces. Keeping this in mind, we designed and synthesized wedge-shaped glycolipids **21**(n, m) (Chart 7) that possess an oligoglycine (1–3 glycine residues) moiety with a terminal amino group at one end and a glucose moiety at the another end.[73] The self-assembly behavior of **21**(n, m) was found to strongly depend on the number of glycine residues (*m*). With increasing the number of glycine residues from $m = 1$ to $m = 3$, the self-assembled morphologies varied from nanofiber to nanotube architectures. The CH deformation (1418 cm^{-1}) and CH skeletal vibration IR bands (1026 cm^{-1}) attributable to polyglycine-II-type hydrogen-bond formation[20,57,58] became remarkable in intensity for the glycolipids **21**(n, 3) with tri-glycine residues at one end. These findings strongly support the structural stabilization of the monolayer membranes by non-covalent hydrogen bonding. In reality, the CH_2 scissoring vibration band in FTIR gave a single peak at 1473 cm^{-1}, suggesting the formation of unsymmetrical monolayer membrane. Detailed electron microscopic observation revealed that the resultant nanotubes possess 7–9 nm inner diameters and 3–4 nm thickness (Figure 11). To the best of our knowledge, the present self-assembled organic nanotube from **21**(11,3) can be recognized as that with the smallest inner diameters among the lipid nanotubes examined so far by electron microscopy.[2] Another unique characteristic is to have a monolayer membrane as well.

6. Single-Head–Single-Tail-Type Peptide Amphiphiles

The self-assembly behavior of peptide bolaamphiphiles **1**(*n*), **2**(*n*), and **3**–**6** with carboxylic terminals has been described in Section **3**. We describe here the self-assembly in water of

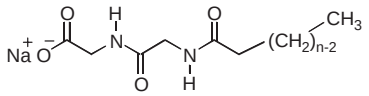

22(n)

Chart 8.

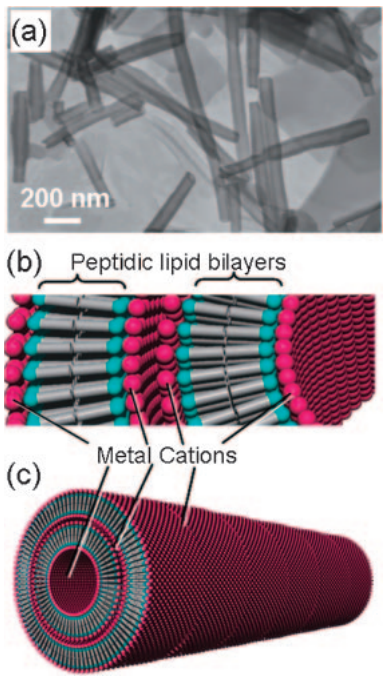

Figure 12. (a) TEM image of metal-coordinated lipid nanotubes from **22**(13) and (b,c) their possible molecular packing.

the sodium salts of single-head–single-tail-type peptide amphiphiles **22**(*n*) (Chart 8), in which the glycylglycine residue is linked to the carboxylic group of saturated fatty acids with different alkyl chain lengths. Just mixing the aqueous solution of **22**(*n*) with diluted acetic acid or with those of transition-metal cations that include copper(II) acetate, manganese(II) acetate, or iron(III) chloride resulted in the perfect self-assembly of organic nanotubes at room temperature and under ambient conditions.[74] The outer and inner diameters of the resultant nanotubes can be regulated from 60 to 500 nm, and from 20 to 150 nm, respectively, strongly depending on the alkyl chain length as well as the metal cations used. For example, the organic nanotubes that self-assembled from both **22**(13) and dilute acetic acid solutions give dimension of 60–80 nm outer diameters and 25–35 nm inner diameters. The combination of **22**(13) with copper(II) acetate produces nanotubes of 100–120 nm in outer diameter and 30–40 nm in inner diameter (Figure 12).

Each peptide amphiphile forms lipid bilayer membranes stabilized by a polyglycine II hydrogen-bond network[20,57,58] among the glycine residues, which stack with 5–30 layers to form the nanotube membrane wall. Furthermore, transition-metal cations such as Cu^{2+} coordinate to the terminal carboxylate anions of the amphiphile, producing a rare example of nanotubes with alternatively stacked layers of both cations

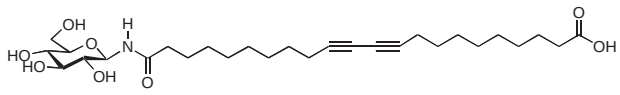

23

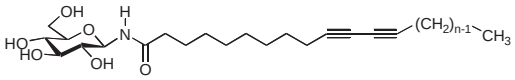

24(n)

Chart 9.

and lipid bilayers (Figures 12b and 12c). It should also be noteworthy that such hybrid nanotubes can function as a self-template to fabricate metal or metal-oxide nanotubes by chemical reduction or calcination since the transition-metal cations distribute in cylindrical layers. In reality, calcination of copper-coordinated organic nanotubes at 500 °C in air was found to produce copper oxide nanotubes efficiently.[74]

7. Glycolipids with a Polymerizable Functional Group

To provide tolerance toward a variety of solvents and heating with organic nanotubes, we attempted to polymerize organic nanotubes by using the self-assembled molecular structure as a matrix. We started by synthesizing the glycolipid **23** (Chart 9) with a polymerizable diacetylenic functional group in the middle of the hydrophobic chain. The glycolipid **23** self-assembled in water to give nanotube structures with 80–120 nm inner diameters before polymerization.[75] The XRD and FTIR analyses revealed that the molecules form an unsymmetrical monolayer membrane with a head-to-tail stacking motif, resulting in parallel molecular packing with a tilt angle of 45°. These features of molecular packing were suitable for topological polymerization of the diacetylenic groups. We therefore tried to polymerize the diacetylenic groups in the resultant nanotube matrix by irradiation of UV light to an aqueous dispersion of the nanotubes. Consequently, the dispersion turned reddish purple, suggesting the formation of polydiacetylenes with the progress of polymerization (Figure 13). Dried glycolipid nanotubes before polymerization melt at 145 °C, whereas the polymerized nanotubes keep the tubular morphology at temperatures below 190 °C. In addition, unpolymerized organic nanotubes dissolve in water as monodispersed molecules at 60 °C, whereas the polymerized nanotubes stably preserve their morphologies even at 100 °C. Similar tolerance toward solvents was also found for the polymerized nanotubes from polymerizable 1-glucosamide glycolipid **24**(*n*) (Chart 9), in which the cis double bond in **12**–**14** was replaced with a diacetylenic group.[76]

8. Control of Self-Assembled Morphology and Length

8.1 Continuous Morphological Control from a Twist to Tubes via Coils. Molecular organization with a variety of molecular building blocks through self-assembly fabricates not only nanometer scaled structures but also templates useful for hybridization with metals, inorganic materials, and biomaterials.[2,77–87] In other words the molecular self-assemblies, with both high aspect ratios and well-regulated dimensions of length, thickness, and diameter within a single nm, can template sol–gel reaction of metal alkoxides. Therefore, if we can

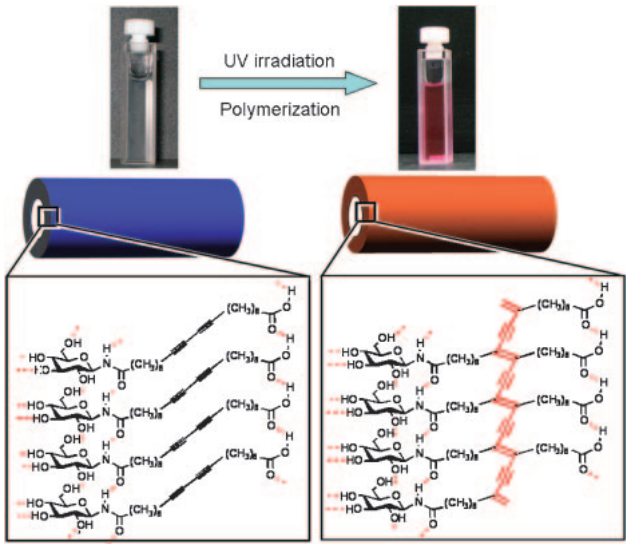

Figure 13. UV polymerization of **23** using a self-assembled nanotube architecture as a reaction matrix.

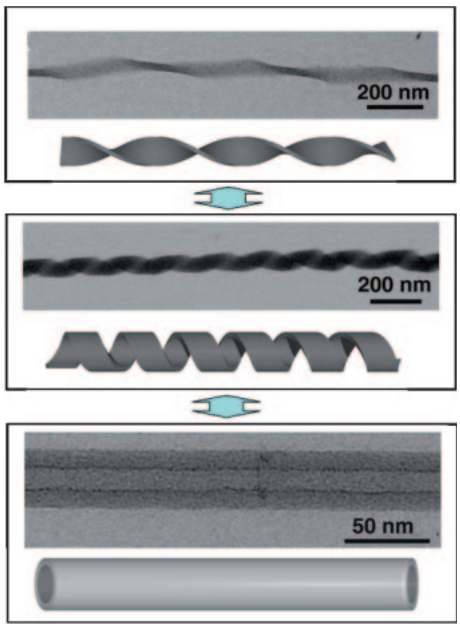

Figure 14. TEM images and each schematic illustration for the self-assembled twist from **7a**, coil from **7b** (after short incubation), and tube morphologies from **7b** (after long incubation).

regulate the dimensions of the organic self-assemblies more precisely and fabricate them, we could produce desirable inorganic or hybridized nanomaterials with well-defined dimensions, which merit application.[87] We found that the saturated **7a** and monoene **7b** components self-assemble into twisted ribbon and nanotube architectures, respectively.[28,30] If both components are ideally mixable and binary self-assembly in any composition is possible, we could produce any one-dimensional structure ranging from a twisted ribbon to tubular morphology as desired. We therefore carried out the binary self-assembly of **7a** with **7b** by continuously changing the mixing compositions. Consequently, the resulting self-assembled morphologies were able to be varied continuously in such a fashion as from a twisted ribbon to tubes via a coiled ribbon (Figure 14).[28] These results mean that by optimizing the composition we can freely produce one-dimensional coiled ribbons as desired.

8.2 Length Control. The technical need for length control of organic nanotubes is great. It is however, still difficult to accomplish length control only by optimizing molecular structures such as the molecular backbone or the position of functional groups. Instead, related research has so far attempted to vary the solvent composition used for self-assembly, or to control the cooling rate around T_{g-l} on self-assembly.[88] We applied gentle mechanical stirring to an aqueous dispersion containing organic nanotubes by using a magnetic stirrer. As a result, stirring at 500 rpm for 6 h was demonstrated to successfully reduce the intrinsic length of several hundred μm nanotubes to 1–10 μm.[89] We found it a facile method to change the stirring rate and time for uniform shortening of the nanotube length.

9. Unique Properties and Encapsulation Functions of Hollow Cylinders

The polarity of confined water in the hollow cylinder of the self-assembled nanotubes from **7** proved to be relatively lower by approximately 20% than that of bulk water, corresponding to that of ethanol.[90] The viscosity of the confined water shows 3–4 cP, corresponding to that of bulk water at −20 °C. That value is 3–4 times as large as that of water at room temperature. Thus, the water in geometrically confined nanospace displays many unique properties different from general bulk water.[90,91] Furthermore, the self-assembled nanotubes from **13** displayed a novel function, encapsulating guest substances with 10–50 nm dimensions into the nanochannel shaped by the hollow cylinders. In particular, capillary action allows us to effectively fill the nanotubes with, for example, gold nanoparticles (1–50 nm),[92,93] cadmium sulfide (2–3 nm),[87] magnetite (ca. 10 nm),[33] spherical protein Ferritin (12 nm),[94] and green fluorescent protein (GFP, 3 × 4.5 nm) (Figure 15). We have also reported that electrostatic interaction between the guests and inner surfaces of the nanotubes is also critical to promote the encapsulation of such guests without depending on capillary force. For example, the self-assembled nanotubes from **20**(18) can possess positive charges in part on the inner surfaces by protonation depending on the pH conditions of the aqueous dispersion. We have demonstrated that such cationic nanotubes efficiently encapsulate negatively charged anionic guests including polymer latex beads (20 nm), Ferritin (Figure 16a), and double-stranded DNA (56 μm long).[32,55] In contrast, the same nanotubes cannot load any positively charged guests like DNA-binding protein from starved cells (Dps, 9 nm) (Figure 16b). Conversely, anionic nanotubes (i.d. = 20 nm) with negatively charged carboxylic acid which self-assembled from **18**(18), can encapsulate Dps (Figure 16c), but not Ferritin (Figure 16d). Interestingly, when using the self-assembled nanotube from **13** with no charges at any surfaces, we found that it can no longer encapsulate guests even by mixing the nanotube and guest solutions. This finding contrasts remarkably with the view that it can do so by capillary action. Very recently, we have succeeded in evaluating the one-dimensional diffusion constant for gold nanoparticles

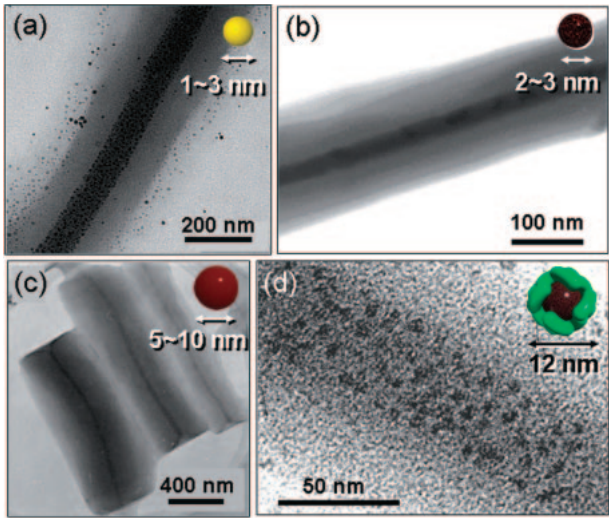

Figure 15. TEM images for the self-assembled lipid nanotubes from **13**, which encapsulate (a) gold nanoparticles, (b) cadmium sulfide, (c) magnetite particles, and (d) ferritin.

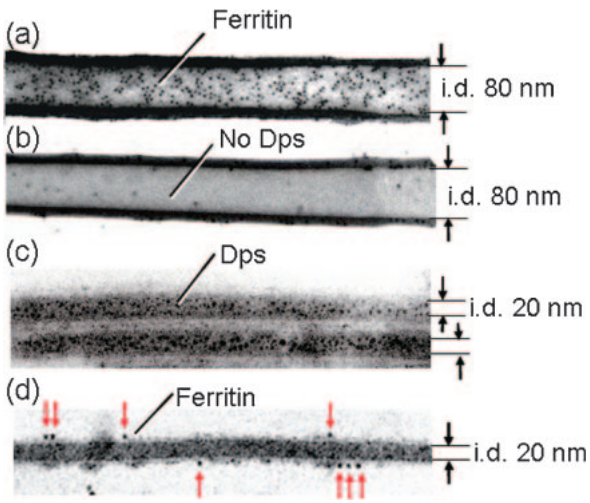

Figure 16. (a) TEM images of the lipid nanotubes from **20**(18) that show effective encapsulation ability for (a) ferritin and (b) no encapsulation of Dps. (c) TEM images of the lipid nanotubes from **18**(18) that show effective encapsulation ability for Dps and (d) no encapsulation of ferritin.

(1.4 nm wide) and Ferritin that diffuse in the confined liquid-phase nanochannel formed by organic nanotubes.[32] The details of the nano-bio applications of a variety of self-assembled nanotubes are reviewed elsewhere.[33]

10. A Massive Production of Organic Nanotubes

It is of great interest to spread self-assembled organic nanotubes into our life through their industrialization. For that purposes, we reconsidered the chemical structures of molecular building blocks in terms of both cost decrease and high safety of starting materials for synthesis. To put it concretely, we focused on the three molecules; the glycolipid **14**, in which the glucose moiety is connected to oleic acid via amide linkage, as well as the peptide lipids **25**(n) (n = 12 and 14) (Chart 10),

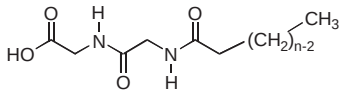

25(n)

Chart 10.

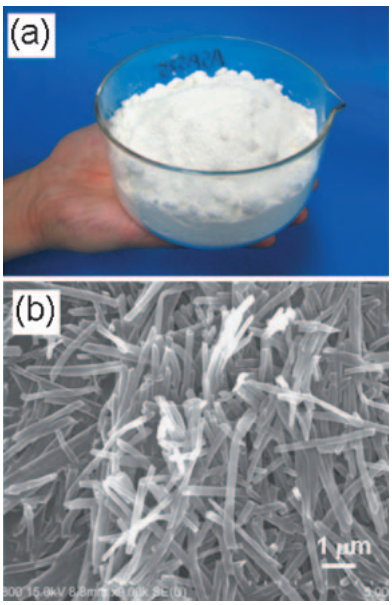

Figure 17. One hundred grams of lipid nanotubes prepared with **14** and the SEM image of the solid powders.

in which glycylglycine moiety is coupled with lauric or myristic acids via amide linkage. Interestingly, after self-assembly of those molecules in alcoholic solvents such as ethanol, we found that evaporation of the solvent for concentration leaves tubular materials as powder solids.[95] Depending on the molecular structures used for self-assembly, the inner diameters were found to range from 40 to 200 nm, outer diameters from 70 to 500 nm, and the length more than several μm. Since organic solvents can well dissolve the tube-forming amphiphiles, one can obtain the nanotubes in quantities thousands greater than those when using the same volume of water (Figure 17). As compared with self-assembly in water, it is completed in a single step and produces organic nanotubes in a short time. We can produce more than 100 g of organic nanotubes in the laboratory and more than 10 kg in a factory setting. The trade mark "organic nanotube AIST®" was registered for three kinds of nanotubes in 2006. Samples of organic nanotubes are currently provided to private enterprise for counter value after making an agreement of material transfer.

11. Future Aspects

A few years ago, it was not an exaggeration to say that nanotubes means carbon nanotubes because of extensive studies and a large number of related achievements. The inner diameters of well-known carbon nanotubes are in the 1–10 nm range and the two terminal ends are generally closed. To accomplish encapsulation experiments, one has to open both ends by harsh chemical reaction.[96] Furthermore, high vacuum and high-temperature conditions, which are not always appro-

priate to load biomolecules into the hollow cylinder, are required to encapsulate some objects. In contrast, self-assembled organic nanotubes are expected to play a leading role in mesoscale host–guest science since they intrinsically possess two opened ends, appropriate flexibility of the membrane wall,[97,98] and tunable surface functionalities.[32,99] To fabricate rationally designed nanotube hosts, one has to take diverse structural factors including functionalities of inner surfaces, the kind and distribution of inner surface charge, the inner diameter, and the nanotube length into consideration. Those factors do not need to be considered in conventional host–guest chemistry using low-molecular weight host compounds like cyclodextrin and cyclophanes. Recently, nanoporous alumina and polycarbonate membranes have been known to template a variety of polymer nanotubes.[100,101] However, the self-assembly procedure, in which a large amount of self-assembled nanotubes form as precipitates after concentration of the solvent used, is much superior to the template method from the viewpoint of a massive production of organic nanotubes. Although there are still many unknown or unresolved issues regarding the properties and formation mechanism, organic nanotubes are of increasing interest.

The author thanks his colleagues Dr. Mitsutoshi Masuda, Dr. Hiroyuki Minamikawa, Dr. Masaki Kogiso, Dr. Masumi Asakawa, Dr. Masaru Aoyagi, Dr. Rika Iwaura, Dr. Bo Yang, and Dr. Qingmin Ji for their continuous support at NARC, AIST, during the course of this work on self-assembled lipid nanotubes. Dr. Naohiro Kameta, Dr. Yong Zhou, Dr. Nahoko Morii, and Dr. Keiko Sumitomo (SORST, JST); Dr. Shoko Kamiya, Dr. Nikolay Goutev, and Dr. George John (CREST, JST) are acknowledged for collaboration on the synthesis and analysis of self-assembled organic tubular architectures. Dr. Kaname Yoshida (Kyoto Univ.), Prof. Tsuguo Sawada, Prof. Kohzo Ito, Dr. Yasuhiro Sakai, Dr. Takuya Fujima, and Dr. Yanli Guo (the University of Tokyo); Prof. Hiroharu Yui (Tokyo Univ. of Science), Prof. Yoshinori Yamaguchi (Waseda Univ.), Prof. Hiroshi Frusawa (Kochi Univ. of Tech.), Prof. Ichiro Yamashita (Nara Inst. Sci. Tech. and CREST, JST), Dr. Yumiko Mishima (CREST, JST), Prof. Kuniaki Nagayama (Natl. Inst. Nat. Sci.), Prof. Jong Hwa Jung (Gyeongsang Natl. Univ.), and Prof. Seiji Shinkai (Kyushu Univ.) are also acknowledged for fruitful collaboration on novel physicochemical and encapsulation properties of LNTs. The Japan Science and Technology Agency (JST) is acknowledged for financial support of the CREST and SORST projects.

References

1 G. Stubbs, *Semin. Virol.*, **1990**, *1*, 405.
2 T. Shimizu, M. Masuda, H. Minamikawa, *Chem. Rev.* **2005**, *105*, 1401.
3 J. H. Fuhrhop, W. Helfrich, *Chem. Rev.* **1993**, *93*, 1565.
4 J. M. Schnur, *Science* **1993**, *262*, 1669.
5 T. Kunitake, *Angew. Chem., Int. Ed. Engl.* **1992**, *31*, 709.
6 S. Iijima, *Nature* **1991**, *354*, 56.
7 S. Iijima, T. Ichihashi, *Nature* **1993**, *363*, 603.
8 P. M. Ajayan, *Chem. Rev.* **1999**, *99*, 1787.
9 C. R. Martin, L. S. V. Dyke, Z. Cai, W. Liang, *J. Am. Chem. Soc.* **1990**, *112*, 8976.
10 M. Steinhart, R. B. Wehrspohn, U. Gösele, J. H. Wendorff, *Angew. Chem., Int. Ed.* **2004**, *43*, 1334.
11 M. A. B. Block, C. Kaiser, A. Khan, S. Hecht, *Top. Curr. Chem.* **2005**, *245*, 89.
12 T. Shimizu, M. Masuda, *J. Am. Chem. Soc.* **1997**, *119*, 2812.
13 M. Masuda, T. Hanada, K. Yase, T. Shimizu, *Macromolecules* **1998**, *31*, 9403.
14 I. Nakazawa, M. Masuda, Y. Okada, T. Hanada, K. Yase, M. Asai, T. Shimizu, *Langmuir* **1999**, *15*, 4757.
15 M. Masuda, T. Hanada, Y. Okada, K. Yase, T. Shimizu, *Macromolecules* **2000**, *33*, 9233.
16 M. Masuda, V. Vill, T. Shimizu, *J. Am. Chem. Soc.* **2000**, *122*, 12327.
17 J. H. Jung, G. John, M. Masuda, K. Yoshida, S. Shinkai, T. Shimizu, *Langmuir* **2001**, *17*, 7229.
18 J. H. Jung, S. Shinkai, T. Shimizu, *Chem.—Eur. J.* **2002**, *8*, 2684.
19 T. Shimizu, M. Kogiso, M. Masuda, *Nature* **1996**, *383*, 487.
20 T. Shimizu, M. Kogiso, M. Masuda, *J. Am. Chem. Soc.* **1997**, *119*, 6209.
21 M. Kogiso, S. Ohnishi, K. Yase, M. Masuda, T. Shimizu, *Langmuir* **1998**, *14*, 4978.
22 T. Shimizu, R. Iwaura, M. Masuda, T. Hanada, K. Yase, *J. Am. Chem. Soc.* **2001**, *123*, 5947.
23 R. Iwaura, K. Yoshida, M. Masuda, K. Yase, T. Shimizu, *Chem. Mater.* **2002**, *14*, 3047.
24 R. Iwaura, K. Yoshida, M. Masuda, M. Ohnishi-Kameyama, M. Yoshida, T. Shimizu, *Angew. Chem., Int. Ed.* **2003**, *42*, 1009.
25 R. Iwaura, F. J. M. Hoeben, M. Masuda, A. P. H. J. Schenning, E. W. Meijer, T. Shimizu, *J. Am. Chem. Soc.* **2006**, *128*, 13298.
26 R. Iwaura, T. Shimizu, *Angew. Chem., Int. Ed.* **2006**, *45*, 4601.
27 T. Shimizu, *Macromol. Rapid Commun.* **2002**, *23*, 311.
28 G. John, J. H. Jung, H. Minamikawa, K. Yoshida, T. Shimizu, *Chem.—Eur. J.* **2002**, *8*, 5494.
29 G. John, J. H. Jung, M. Masuda, T. Shimizu, *Langmuir* **2004**, *20*, 2060.
30 G. John, M. Masuda, Y. Okada, K. Yase, T. Shimizu, *Adv. Mater.* **2001**, *13*, 715.
31 M. Masuda, T. Shimizu, *Langmuir* **2004**, *20*, 5969.
32 N. Kameta, M. Masuda, H. Minamikawa, Y. Mishima, I. Yamashita, T. Shimizu, *Chem. Mater.* **2007**, *19*, 3553.
33 T. Shimizu, *J. Polym. Sci., Part A* **2008**, *46*, 2601.
34 M. Numata, T. Matsumoto, M. Umeda, K. Koumoto, K. Sakurai, S. Shinkai, *Bioorg. Chem.* **2003**, *31*, 163.
35 T. Hasegawa, T. Fujisawa, M. Numata, M. Umeda, T. Matsumoto, T. Kimura, S. Okumura, K. Sakurai, S. Shinkai, *Chem. Commun.* **2004**, 2150.
36 M. Numata, C. Li, A. H. Bae, K. Kaneko, K. Sakurai, S. Shinkai, *Chem. Commun.* **2005**, 4655.
37 T. Matsumoto, M. Umeda, T. Hasegawa, M. Numata, K. Sakurai, K. Koumoto, S. Shinkai, *J. Am. Chem. Soc.* **2005**, *127*, 5875.
38 M. Numata, T. Hasegawa, T. Fujisawa, K. Sakurai, S. Shinkai, *Org. Lett.* **2004**, *6*, 4447.
39 T. Hasegawa, S. Haraguchi, M. Numata, C. Li, A.-H. Bae, T. Fujisawa, K. Kaneko, K. Sakurai, S. Shinkai, *Org. Bioorg. Chem.* **2005**, *3*, 4321.

40 M. R. Ghadiri, J. R. Granja, R. A. Milligan, D. E. McRee, N. Khazanovich, *Nature* **1993**, *366*, 324.
41 M. R. Ghadiri, J. R. Granja, L. K. Buehler, *Nature* **1994**, *369*, 301.
42 D. T. Bong, T. D. Clark, J. R. Granja, M. R. Ghadiri, *Angew. Chem., Int. Ed.* **2001**, *40*, 988.
43 A. Harada, J. Li, M. Kamachi, *Nature* **1993**, *364*, 516.
44 A. Harada, J. Li, M. Kamachi, *J. Am. Chem. Soc.* **1994**, *116*, 3192.
45 H. Fenniri, P. Mathivanan, K. L. Vidale, D. Sherman, K. Hallenga, K. V. Wood, J. G. Stowell, *J. Am. Chem. Soc.* **2001**, *123*, 3854.
46 N. Kimizuka, T. Kawasaki, K. Hirata, T. Kunitake, *J. Am. Chem. Soc.* **1995**, *117*, 6360.
47 V. Percec, C.-H. Ahn, G. Ungar, D. J. P. Yeardley, M. Möller, S. S. Sheiko, *Nature* **1998**, *391*, 161.
48 J. N. Israelachivili, *Intermolecular and Surface Forces*, Academic Press, Inc., New York, **1985**.
49 J.-H. Fuhrhop, J. Koening, in *Monographs in Supramolecular Chemistry*, ed. by J. F. Stoddart, The Royal Society of Chemistry, Cambridge, **1994**.
50 N. Nakashima, S. Asakuma, T. Kunitake, *J. Am. Chem. Soc.* **1985**, *107*, 509.
51 M. S. Spector, K. R. K. Easwaran, G. Jyothi, J. V. Selinger, A. Singh, J. M. Schnur, *Proc. Natl. Acad. Sci. U.S.A.* **1996**, *93*, 12943.
52 M. S. Spector, J. V. Selinger, J. M. Schnur, in *Topics in Stereochemistry*, ed. by M. M. Green, R. J. M. Nolte, E. W. Meijer, **2003**, Vol. 24, p. 281.
53 K. Yamada, H. Ihara, T. Ide, T. Fukumoto, C. Hirayama, *Chem. Lett.* **1984**, 1713.
54 P. Yager, P. E. Schoen, *Mol. Cryst. Liq. Cryst.* **1984**, *106*, 371.
55 N. Kameta, M. Masuda, H. Minamikawa, N. V. Goutev, J. A. Rim, J. H. Jung, T. Shimizu, *Adv. Mater.* **2005**, *17*, 2732.
56 T. Shimizu, S. Ohnishi, M. Kogiso, *Angew. Chem., Int. Ed. Engl.* **1998**, *37*, 3260.
57 F. H. C. Crick, A. Rich, *Nature* **1955**, *176*, 780.
58 M. Kogiso, M. Masuda, T. Shimizu, *Supramol. Chem.* **1998**, *9*, 183.
59 M. Kogiso, Y. Okada, T. Hanada, K. Yase, T. Shimizu, *Biochim. Biophys. Acta* **2000**, *1475*, 346.
60 M. Kogiso, Y. Okada, K. Yase, T. Shimizu, *J. Colloid Interface Sci.* **2004**, *273*, 394.
61 J. H. P. Tyman, *Chem. Soc. Rev.* **1979**, *8*, 499.
62 J. H. Jung, G. John, K. Yoshida, T. Shimizu, *J. Am. Chem. Soc.* **2002**, *124*, 10674.
63 J. H. Jung, Y. Do, Y.-A. Lee, T. Shimizu, *Chem.—Eur. J.* **2005**, *11*, 5538.
64 S. Kamiya, H. Minamikawa, J. H. Jung, B. Yang, M. Masuda, T. Shimizu, *Langmuir* **2005**, *21*, 743.
65 K. Yoshida, H. Minamikawa, S. Kamiya, T. Shimizu, S. Isoda, *J. Nanosci. Nanotechnol.* **2007**, *7*, 960.
66 H. Yui, H. Minamikawa, R. Danev, K. Nagayama, S. Kamiya, T. Shimizu, *Langmuir* **2008**, *24*, 709.
67 J. M. Schnur, B. R. Ratna, J. V. Selinger, A. Singh, G. Jyothi, K. R. K. Easwaran, *Science* **1994**, *264*, 945.
68 M. S. Spector, R. R. Price, J. M. Schnur, *Adv. Mater.* **1999**, *11*, 337.
69 M. Masuda, T. Shimizu, *Chem. Commun.* **2001**, 2442.
70 T. Shimizu, *J. Polym. Sci., Part A* **2006**, *44*, 5137.
71 M. Masuda, K. Yoza, T. Shimizu, *Carbohydr. Res.* **2005**, *340*, 2502.
72 N. Kameta, M. Masuda, H. Minamikawa, T. Shimizu, *Langmuir* **2007**, *23*, 4634.
73 N. Kameta, G. Mizuno, M. Masuda, H. Minamikawa, M. Kogiso, T. Shimizu, *Chem. Lett.* **2007**, *36*, 896.
74 M. Kogiso, Y. Zhou, T. Shimizu, *Adv. Mater.* **2007**, *19*, 242.
75 M. Masuda, S. Masubuchi, T. Shimizu, Preprints of The CSJ Spring Meeting, **2005**, p. 1.
76 S. Kamiya, T. Shimizu, *Polym. Prepr. Jpn.* **2005**, *54*, 4799.
77 J. H. Jung, H. Kobayashi, M. Masuda, T. Shimizu, S. Shinkai, *J. Am. Chem. Soc.* **2001**, *123*, 8785.
78 J. H. Jung, S. Shinkai, T. Shimizu, *Nano Lett.* **2002**, *2*, 17.
79 J. H. Jung, H. Kobayashi, K. J. C. v. Bommel, S. Shinkai, T. Shimizu, *Chem. Mater.* **2002**, *14*, 1445.
80 K. J. C. v. Bommel, A. Friggeri, S. Shinkai, *Angew. Chem., Int. Ed.* **2003**, *42*, 980.
81 J. H. Jung, S. Shinkai, T. Shimizu, *Chem. Rec.* **2003**, *3*, 212.
82 Q. Ji, R. Iwaura, M. Kogiso, J. H. Jung, K. Yoshida, T. Shimizu, *Chem. Mater.* **2004**, *16*, 250.
83 Q. Ji, T. Shimizu, *Chem. Commun.* **2005**, 4411.
84 Y. Zhou, Q. Ji, M. Masuda, S. Kamiya, T. Shimizu, *Chem. Mater.* **2006**, *18*, 403.
85 Q. Ji, R. Iwaura, T. Shimizu, *Chem. Mater.* **2007**, *19*, 1329.
86 Y. Zhou, M. Kogiso, C. He, Y. Shimizu, N. Koshizaki, T. Shimizu, *Adv. Mater.* **2007**, *19*, 1055.
87 Y. Zhou, T. Shimizu, *Chem. Mater.* **2008**, *20*, 625.
88 B. N. Thomas, C. R. Safinya, R. J. Plano, N. A. Clark, *Science* **1995**, *267*, 1635.
89 B. Yang, S. Kamiya, H. Yui, M. Masuda, T. Shimizu, *Chem. Lett.* **2003**, *32*, 1146.
90 H. Yui, Y. Guo, K. Koyama, T. Sawada, G. John, B. Yang, M. Masuda, T. Shimizu, *Langmuir* **2005**, *21*, 721.
91 Y. Guo, H. Yui, H. Minamikawa, M. Masuda, S. Kamiya, T. Sawada, K. Ito, T. Shimizu, *Langmuir* **2005**, *21*, 4610.
92 B. Yang, S. Kamiya, K. Yoshida, T. Shimizu, *Chem. Commun.* **2004**, *5*, 500.
93 B. Yang, S. Kamiya, Y. Shimizu, N. Koshizaki, T. Shimizu, *Chem. Mater.* **2004**, *16*, 2826.
94 H. Yui, Y. Shimizu, S. Kamiya, I. Yamashita, M. Masuda, K. Ito, T. Shimizu, *Chem. Lett.* **2005**, *34*, 232.
95 M. Asakawa, T. Shimizu, *Expected Mater. Future* **2007**, *7*, 38.
96 S. C. Tsang, Y. K. Chen, P. J. F. Harris, M. L. H. Green, *Nature* **1994**, *372*, 159.
97 H. Frusawa, A. Fukagawa, Y. Ikeda, J. Araki, K. Ito, G. John, T. Shimizu, *Angew. Chem., Int. Ed.* **2003**, *42*, 72.
98 T. Fujima, H. Frusawa, H. Minamikawa, K. Ito, T. Shimizu, *J. Phys.: Condens. Matter* **2006**, *18*, 3089.
99 N. Kameta, M. Masuda, G. Mizuno, N. Morii, T. Shimizu, *Small* **2008**, *4*, 561.
100 C. Y. R. Martin, *Science* **1994**, *266*, 1961.
101 Y. Guo, H. Yui, H. Minamikawa, B. Yang, M. Masuda, K. Ito, T. Shimizu, *Chem. Mater.* **2006**, *18*, 1577.

Toshimi Shimizu received his B.S. and M.S. degrees in Polymer Chemistry from Kyoto University, Japan in 1975 and 1977, respectively, and obtained his Ph.D. degree from Kyoto University, Japan in 1983. In 1977, he joined the Research Institute of Polymers and Textiles, Agency of Industrial Science and Technology (AIST), MITI. After his postdoctoral research at the Free University of Berlin with Prof. J.-H. Fuhrhop, he joined the National Institute of Materials and Chemical Research, AIST, MITI in 1993. From 2001 to 2008, he served as the director of the Nanoarchitectonics Research Center, AIST. He has been promoting the CREST and SORST projects by Japan Science and Technology Corporation (JST) as a project director. He is currently research coordinator (nanotechnology, materials, and manufacturing) of AIST and serving concurrently as a deputy director of the Nanotube Research Center (NTRC), AIST. His research focuses on the noncovalent synthesis of high-axial-ratio nanostructures through the self-assembly of amphiphilic monomers. In particular, he is now engaged in developing organic nanotube materials. He is the recipient of the Minister's Award of MITI, 2000, The Award of the Society of Polymer Science 2001, Japan, and The Chemical Society of Japan (CSJ) Award for Creative Work for 2006.